Original Article

JCBFM

Journal of Cerebral Blood Flow & Metabolism
2020, Vol. 40(3) 639–655

DOI: 10.1177/0271678X19830791
journals.sagepub.com/home/jcbfm
SAGE

TGFα preserves oligodendrocyte lineage cells and improves white matter integrity after cerebral ischemia

Xuejiao Dai[1,2], Jie Chen[1], Fei Xu[1,3], Jingyan Zhao[1], Wei Cai[1], Zeyu Sun[1], T Kevin Hitchens[4,5], Lesley M Foley[4], Rehana K Leak[6], Jun Chen[1,3] and Xiaoming Hu[1,3]

Abstract

Transforming growth factor α (TGF-α) has been reported to play important roles in neurogenesis and angiogenesis in the injured brain. The present study characterizes a novel role for TGFα in oligodendrocyte lineage cell survival and white matter integrity after ischemic stroke. Three days after transient (60 min) middle cerebral artery occlusion (tMCAO), TGFα expression was significantly increased in microglia/macrophages and neurons. Expression of the receptor of TGFα—epidermal growth factor receptor (EGFR)—was increased in glial cells after ischemia, including in oligodendrocyte lineage cells. TGFα knockout enlarged brain infarct volumes and exacerbated cell death in oligodendrocyte precursor cells (OPCs) and oligodendrocytes three days after tMCAO. TGFα-deficient mice displayed long-term exacerbation of sensorimotor deficits after tMCAO, and these functional impairments were accompanied by loss of white matter integrity and impaired oligodendrocyte replacement. In vitro studies confirmed that 5 or 10 ng/mL TGFα directly protected OPCs and oligodendrocytes against oxygen and glucose deprivation (OGD)-induced cell death, but exerted no effects on OPC differentiation. Further studies identified STAT3 as a key transcription factor mediating the effects of TGFα on OPCs and oligodendrocytes. In conclusion, TGFα provides potent oligodendrocyte protection against cerebral ischemia, thereby maintaining white matter integrity and improving neurological recovery after stroke.

Keywords

Transforming growth factor α, white matter, oligodendrocyte, cell death, stroke, STAT3

Received 15 November 2018; Revised 16 January 2019; Accepted 17 January 2019

Introduction

The occlusion of large blood vessels, such as the middle cerebral artery (MCA), results in ischemic brain tissue damage spanning both gray and white matter. White matter is mainly comprised of myelinated and unmyelinated axons, myelin-producing oligodendrocytes, and other glial cells.[1] White matter components are highly sensitive to ischemic insults at all stages of development,[2,3] and their vulnerability increases further with age.[4] In the adult brain, injured white matter is observed within days after ischemic stroke, and manifested as oligodendrocyte abnormalities and loss of the myelin sheath.[2] This early-onset damage persists and evolves over time, resulting in secondary axonal degeneration and impaired nerve conductivity. The resulting loss of white matter integrity contributes to long-term

[1]Department of Neurology, Pittsburgh Institute of Brain Disorders and Recovery, University of Pittsburgh School of Medicine, Pittsburgh, USA
[2]Xiangya School of Medicine, Central South University, Changsha, China
[3]Geriatric Research, Education and Clinical Center, Veterans Affairs Pittsburgh Health Care System, Pittsburgh, USA
[4]Animal Imaging Center, School of Medicine, University of Pittsburgh, Pittsburgh, USA
[5]Department of Neurobiology, School of Medicine, University of Pittsburgh, Pittsburgh, USA
[6]Graduate School of Pharmaceutical Sciences, Duquesne University, Pittsburgh, USA

Corresponding author:
Xiaoming Hu, Department of Neurology, University of Pittsburgh School of Medicine, 200 Lothrop Street, SBST 506, Pittsburgh, PA 15213, USA.
Email: hux2@upmc.edu

functional and cognitive deficits after stroke.[2,5,6] Ischemic brain injury engages endogenous repair mechanisms that attempt to reestablish the integrity of white matter by preservation of pre-existing oligodendrocytes and the repopulation of myelin-forming oligodendrocytes from oligodendrocyte precursor cells (OPCs).[7–9] However, OPCs and oligodendrocytes are highly sensitive to ischemia-induced oxidative stress and excitotoxicity.[10–12] Conspicuous swelling of oligodendrocytes can be observed within 30 min after ischemia,[2] and large numbers of oligodendrocytes are lethally injured within 3 h after stroke.[2] The death of oligodendrocytes and OPCs results in long-term myelin loss, axonal injury, and inadequate remyelination. Therefore, therapies that maintain oligodendrocyte and OPC viability after ischemic injury have the potential to improve long-term neurological recovery after stroke, and identification of the underlying mechanisms might accelerate the discovery of novel drug targets in the future.

Transforming growth factor α (TGF-α), a member of the epidermal growth factor (EGF) family, is structurally homologous to EGF and binds to the EGF receptor (EGFR).[13] Previous studies have demonstrated that both TGFα and EGFR are highly expressed in the central nervous system (CNS).[14,15] TGFα is a particularly prominent ligand for EGFR in the CNS due to its widespread distribution and high abundance compared to other EGFR ligands.[14,15] TGFα plays important roles in neural cell proliferation[16] and differentiation[17] and stimulates the synthesis of nerve growth factor in astrocytes.[18] Intranasal or intracerebral injection of TGFα has been shown to reduce infarct volume[19,20] and mitigate behavioral deficits[21] in experimental models of stroke. Mechanistic studies have further shown that TGFα inhibits cell death signaling[22] and promotes neurogenesis and angiogenesis after ischemic stroke.[23–25] Although the expression of EGFR in oligodendrocyte linage cells has been reported,[26,27] the effects of TGFα on white matter injury after stroke have, to our knowledge, not been investigated.

The present study investigates the role of TGFα in white matter integrity in the transient MCA occlusion (tMCAO) murine model of stroke. Within three days after experimental stroke, we observed elevated TGFα production from microglia and neurons, a response accompanied by the induction of the EGFR receptor in oligodendrocyte lineage as well as other CNS cells. TGFα deficiency exacerbated tissue damage not only in gray matter but also in white matter and promoted long-term neurological dysfunction. TGFα knockout (KO) mice also displayed prominent loss of oligodendrocytes and their precursor cells. In vivo and in vitro studies revealed that TGFα protects oligodendrocyte lineage cells from ischemic injury and that activation of STAT3 signaling plays a critical role in TGFα-afforded protection of oligodendrocytes. Thus, TGFα has the potential to serve as a therapeutic target in the quest to improve white matter integrity after stroke.

Materials and methods

Animals

All animal experiments were approved by the University of Pittsburgh Institutional Animal Care and Use Committee, performed in accordance with the National Institutes of Health *Guide for the Care and Use of Laboratory Animal*, and reported in accordance with the ARRIVE guidelines (*Animal Research: Reporting in Vivo Experiments*). Wild-type (WT) and TGFα KO C57BL/6 mice (8–12 weeks old) were obtained from the Jackson Laboratory. All mice were housed in a specific pathogen-free facility with a 12-h light/dark cycle. All efforts were made to minimize animal suffering and the number of animals used.

Murine model of transient focal ischemia

All animals were randomly assigned to experimental groups using a lottery drawing box. Animals were anesthetized with 1.5% isoflurane in a 30% O_2/68.5% N_2O mixture under spontaneous breathing conditions. Transient focal ischemia was induced by intraluminal occlusion of the left MCA for 60 min with silicone-coated sutures. Rectal temperature was maintained at $37.0^{\circ}C \pm 0.5^{\circ}C$ and monitored with a rectal thermometer. Regional cerebral blood flow (rCBF) was monitored in all stroke animals using laser Doppler flowmetry or two-dimensional laser speckle imaging system. Animals that died or failed to display an rCBF reduction to 25% of the baseline using laser Doppler flowmetry were excluded from further analyses. Sham-operated mice underwent the same anesthesia and artery exposure without ischemia induction. The tMCAO or sham surgeries were performed by an investigator blinded to genotypes. A final tally of 154 mice (25 sham-operated and 129 ischemic mice) were used in this study, including 35 mice that were excluded from further assessments, either because of death (33) after ischemia or failure of ischemia induction (2). The mortality during tMCAO was 15.9% (7 of 44) in WT male mice, 33.8% (22 of 65) in TGFα KO male mice, 10% (1 of 10) in female WT mice, and 30% (3 of 10) in female TGFα KO mice.

Ovariectomy

Ovariectomy (OVX) was performed on female mice (8–12 weeks old), as previously described.[28] In brief, animals were anesthetized with 1.5% isoflurane in a 30%

O_2/68.5% N_2O mixture under spontaneous breathing conditions. Following anesthesia, two bilateral incisions were made in the skin 1 cm from the midline between the last costal margin and the thigh, followed by an incision in the muscle. The peritoneal cavity was exposed for the removal of the ovaries and bilateral ligation of the uterine tubes. After the procedure, the muscles and the skin were sutured and rinsed. Surgeries to induce tMCAO were performed two weeks after OVX. Female mice are commonly used at two weeks after OVX in stroke studies to mimic the low estrogen conditions of menopause.[29,30] A previous study reported that the estrogen levels in female mice dropped below detection limit within two weeks after OVX.[30]

Cortical CBF measurements

rCBF was measured using the two-dimensional laser speckle imaging system (PeriCam PSI System) or laser doppler flowmetry, as described previously.[31] WT or TGFα KO male mice were subjected to repeated measurements of rCBF before and during tMCAO as well as 10 min after reperfusion. CBF changes were expressed as a percentage of pre-MCAO baseline values.

Neurological deficit scores

Neurological deficit was assessed by a blinded investigator using a six-point-scale neurological score (0, no observable deficit; 1, torso flexion to right; 2, spontaneous circling to right; 3, leaning/falling to right; 4, no spontaneous movement; 5, death).

Measurements of tissue loss and *myelin basic protein* loss

A series of six sections spanning the MCA territory was selected from each mouse brain and stained with an antibody for the neuron-specific marker microtubule associated protein 2 (MAP2) or myelin basic protein (MBP), a marker of viable white matter. Loss of $MAP2^+$ or MBP^+ tissue was measured by a blinded observer with NIH ImageJ software. Tissue loss was calculated as the volume of the contralateral hemisphere minus the non-infarcted volume of the ipsilateral hemisphere, a formula that controls for edema at the site of injury.

Immunofluorescence staining and quantification

Brains were excised from the skull following cardiac perfusion with saline and 4% paraformaldehyde (Sigma-Aldrich) in phosphate-buffered saline (PBS). Brains were then dehydrated in 30% sucrose in PBS and 25-μm thick brain sections were cut on a freezing microtome and subjected to immunofluorescent staining. Primary antibodies included the following: mouse anti-TGFα (Abcam), goat anti-Iba1 (Abcam), rabbit anti-NeuN (Millipore), rabbit anti-GFAP (DAKO), mouse anti-NG2 (Millipore), mouse anti-APC (Millipore), rabbit anti-MAP2 (Santa Cruz Biotechnology), mouse anti-PDGFRα (R&D Systems), rabbit anti-MBP (Abcam), mouse anti-SMI32 (non-phosphorylated neurofilament H monoclonal, BioLegend), mouse anti-CASPR (Millipore), rabbit anti-Nav1.6 (Alomone), rat anti-BrdU (Abcam). TUNEL staining (fluorescein) was performed with the In Situ Cell Death Detection Kit (Roche). Sections were mounted with DAPI Fluoromount-G (Southern Biotech). Cell death in culture was detected by the LIVE/DEAD Viability/Cytotoxicity Kit (Invitrogen). Immunostaining images were captured by confocal microscopy (Olympus). All images were processed with ImageJ by a blinded observer. The average numbers of positively stained cells were calculated from two microscopic fields in the external capsule (EC), two fields in the cortex, and two fields in the striatum of each section. Two sections were analyzed for each brain.

For the measurements of MBP and SMI32 staining intensity, regions of interest (ROIs) were drawn in the striatum, cortex, and EC. The average staining intensity was calculated from two randomly selected microscopic fields in each region, and two sections were analyzed for each brain.

For the measurement of corpus callosum (CC)/EC width, the ipsilateral and contralateral CC and EC were divided into 10 equal segments. The width of each segment was measured and normalized to the length at the midline.

Magnetic resonance imaging

Perfusion-fixed brains were left in the skull and imaged ex vivo using a Bruker AV3HD 11.7 Tesla (T)/89 mm vertical-bore microimaging system equipped with a Micro2.5 gradient set capable of 1500 mT/m, a 20-mm quadrature radio freqency (RF) resonator and ParaVision 6.0.1 (Bruker Biospin). Diffusion tensor imaging (DTI) data were collected using a multislice spin-echo sequence with 5 A0 images and 30 non-colinear diffusion images with the following parameters: TE/TR 22/2800 ms, 2 averages, 160×160 matrix, 16×16 mm field of view, 25 slices, 0.5 mm slice thickness, b-value = 3000 s/mm^2, and $\Delta/\delta = 11.0/5.0$ ms. DTI data were analyzed with DSI Studio software (http://dsi-studio.labsolver.org/). ROIs were manually drawn to encompass the EC in the ipsilesional and contralesional hemispheres and used to determine fractional anisotropy (FA), axial diffusivity (AD), and radial diffusivity (RD) by a blinded observer. Directionally encoded color (DEC), FA, and RD maps were generated

by DSI Studio software. Data were expressed as ratio of values of ipsilateral/contralateral hemisphere.

Behavioral tests

The adhesive removal test. This text was performed by a blinded observer to assess tactile response and sensorimotor function. Adhesive tapes (2×3 mm) were applied to the forepaws contralateral to the injured hemisphere. Tactile responses were measured as the time to initially contact the contralateral paws and the time to remove the adhesive tape. The maximal observation period was set to 120 s.

Rotarod test. Motor coordination and balance were tested on an accelerating Rotarod (IITC Life Science). Mice were placed on an accelerated rotating rod with the speed increasing from 4 to 40 r/min within 2 min (female) or 5 min (male). Mice were trained for three trials per day from three days before tMCAO and tested three times daily with an intermission of 5 min at the indicated time points after stroke. The total time spent on the accelerating rod before falling off was recorded automatically. The averages of three trials on the final day of training were recorded as the pre-surgery baseline value. After surgery, the average latency to fall off the rotating rod during three trials was recorded on the days indicated in the graph.

Foot-fault test. Mice were placed on a stainless-steel grid floor ($20\,\text{cm} \times 40\,\text{cm}$ with a mesh size of $4\,\text{cm}^2$) and videotaped for a 1-min-long observation period. The total number of steps during this interval was counted by a blinded observer. The number of foot-faults (i.e. when the forelimb fell through the grid) was also recorded. The data are expressed as the percentages of errors out of total steps recorded.

Flow cytometry and ImageStream

Single-cell suspensions were prepared from tMCAO or sham brains using the Neural Tissue Dissociation Kit (Miltenyi Biotec), according to the manufacturer's instructions. Cells and myelin were stratified on a 30–70% Percoll gradient (GE Healthcare BioSciences). Cells at the interface were collected and stained with fluorophore-labeled anti-mouse CD45-PB (eBioscience), CD11b-BV605 (BD Bioscience), O4-APC (Millipore), glial glutamate aspartate transporter-PE (GLAST; Miltenyi Biotec), EGFR-FITC (Abcam), and the appropriate isotype controls (Abcam). For EGFR staining in neurons, cells were stained with EGFR-FITC (Abcam), permeabilized and fixed with the intracellular staining kit (eBioscience), and then stained with MAP2 (Santa Cruz Biotechnology) followed by anti-IgG-APC (R&D Systems). Flow cytometric analysis was performed using an FACS flow cytometer (BD Biosciences). Fluorochrome compensation was performed with single stained OneComp eBeads (Thermo Fisher eBioscience). ImageStream analysis was performed using an ImageStream®X Mark II Imaging Flow Cytometer (Millipore), which produces high-resolution images of single cells directly in flow with sensitivity exceeding conventional flow cytometers. Six thousand cells were collected in each sample. Data analysis was performed using IDEAS software (Millipore).

Primary OPC and oligodendrocyte cultures

Primary OPC cultures were isolated with the differential attachment method, as described previously.[32] Briefly, brains of P1-2 mixed-sex Sprague Dawley rat pups were triturated after removing the meninges and blood vessels. The brain tissues were dissociated with Trypsin (0.01%) at 37°C for 15 min. After washing with ice-cold Dulbecco's Modified Eagle Medium (DMEM), cells were passed through a 70 μm filter and plated onto poly-D-lysine-coated T-flasks filled with culture media (DMEM/F12 containing 10% heat-inactivated Fetal Bovine Serum (FBS), 2 mM L-glutamine, 1 mM sodium pyruvate, 100 μM nonessential amino acids, 50 U/mL penicillin, and 50 μg/mL streptomycin).[33] Cells were grown to confluence (12–14 days in vitro (DIV)) in a humidified incubator at 37°C and with 5% CO_2. Microglia were removed by shaking the mixed glia-containing flasks for 1 h at 180 r/min. After removing the microglia, the flasks were subjected to shaking at 200 r/min overnight to separate OPCs from the astrocyte layer.[34] OPCs were maintained for 5–9 days in a serum-free basal defined medium (BDM: DMEM, 0.1% bovine serum albumin, 50 μg/mL human apo-transferrin, 50 μg/mL insulin, 30 nM sodium selenite, 10 nM D-biotin, 10 nM hydrocortisone) containing 10 ng/mL PDGF and 10 ng/mL bFGF. For oligodendrocyte induction, OPCs were stimulated with T3 and CNTF (10 ng/mL) for seven days. The medium was exchanged every two days.

Oxygen–glucose deprivation and treatment

To model ischemia in vitro, OPCs or oligodendrocyte cultures were incubated in oxygen–glucose deprivation (OGD) medium (120 mM NaCl, 5.4 mM KCl, 1.8 mM CaCl, 0.8 mM MgCl, 25 mM TrisHCl, pH = 7.4), and cultures were placed in a Billups-Rothenberg modular incubator chamber. The chamber was first flushed for 5 min with 95% N_2 and 5% CO_2 and then sealed. The chamber was placed in a 37°C incubator (Forma, Thermo Fisher Scientific) for 2 h and was then returned to 95% air, 5% CO_2 with normal glucose medium for 24 h. Control

cultures seeded in parallel were incubated for the same duration at 37°C in humidified 95% air and 5% CO_2.

OPCs or oligodendrocytes were treated with TGFα (1.25, 2.5, 5, 10, and 20 ng/mL) or control medium for 24 h after 2 h OGD. Cell survival was assessed by the MTT (3-(4,5-dimethyl-2-thiazolyl)-2,5-diphenyl-2-H-tetrazolium bromide) assay (Thermo Fisher Scientific), lactate dehydrogenase (LDH) assay (Point Scientific), and the Live/Dead staining kit (Invitrogen), according to manufacturers' protocols. For immunostaining, cells were fixed with 4% paraformaldehyde and stained with mouse anti-NG2 (Millipore) or rabbit anti-MBP (Abcam), followed by TUNEL (Roche) staining. Dead or dying cells were defined as $TUNEL^+$ cells. Images were processed with NIH ImageJ software by a blinded observer for the counting of automatically recognized cells.

Western blots

Cells were pelleted, washed with pre-cold PBS, and homogenized in 300 μL RIPA buffer (with Protease and Phosphatase Inhibitor Cocktail, ThermoFisher Scientific). Thirty grams of protein per sample were loaded on a 10% Precast Protein gel (BioRad). Proteins were transferred to a Polyvinylidene Fluoride (PVDF) membrane, and nonspecific binding was blocked with 5% milk (in Phosphate Buffered Saline Tween (PBST)) for 1 h at room temperature. The membrane was then incubated with primary antibodies against pSTAT3 (rabbit, 1:500; Cell Signaling), and total STAT3 protein (mouse, 1:1000; Cell Signaling) overnight at 4°C. Proteins were stained with species-specific HRP-linked antibodies (1:2000; Cell Signaling) and scanned by gel densitometry scanning. Protein expression was normalized to total STAT3 and expressed as a percentage of the OGD control group.

Real time polymerase chain reaction

Total RNA was isolated from cultured OPCs using the RNeasy Mini Kit (QIAGEN) according to the manufacturer's instructions. One microgram of RNA was used to synthesize the first strand of cDNA using the Superscript First-Strand Synthesis System for real time polymerase chain reaction (RT-PCR) (Invitrogen). Polymerase chain reaction (PCR) was performed on the Option 2 Real-Time PCR Detection System (Bio-Rad) using primers (MBP—Forward: CACAGAAGA GACCCTCACAGCGACA, Reverse: CCGCTAAAG AAGCGCCCGATGGA; MOG—Forward: GCCGT GGAGTTGAAAGTAGAAGA, Reverse: ATAGGC ACAAGGGCAATGAGA; MAG—Forward: GCTG GGAGGGAAATACTATTTCC, Reverse: GACGCT GTCCTCTGAGAAGGA; GAPDH—Forward: TGC TGGTGCTGAGTATGTCGTG, Reverse: CGGAG ATGATGACCCTTTGG) and SYBR green PCR Master Mix (QIAGEN).

Statistical analyses

All data were reported as the mean ± SD. The two-tailed Student's t test was used for the comparison of two groups when the data were normally distributed and variances were equal. The Mann–Whitney U test was used for continuous variables with non-normal distributions. Differences across multiple groups were analyzed using a one-way ANOVA when data were normally distributed and variances were equal. A repeated-measure ANOVA was used to compare data from many groups with multiple measurements over time. A post hoc Bonferroni's test was used for pairwise comparisons between means. Spearman rank correlation analyses were applied to non-normally distributed data. In all analysis, $p \leq 0.05$ was considered statistically significant.

Results

Cerebral ischemic injury induces an elevation of neuronal and microglial/macrophage TGFα within three days

We commenced this study by examining the expression of TGFα in CNS cells with immunofluorescent staining. Expression of TGFα in sham brains was undetectable (Supplemental Figure 1(A)). However, ischemic injury induced a robust increase in TGFα expression in $NeuN^+$ neurons and $Iba1^+$ microglia/macrophages three days after tMCAO (Figure 1(a)). In contrast, no TGFα signal was detected in $GFAP^+$ astrocytes, $NG2^+$ OPCs, or APC^+ oligodendrocytes (Figure 1(b)). An ImageStream flow cytometer was then used to image the signal of TGFα in single cells labeled with various fluorescent markers. The results confirmed that the expression of TGFα increased significantly in $MAP2^+$ neurons and $CD45^+CD11b^+$ microglia/macrophages three days after stroke (Figure 1(c) to (e), Supplemental Figure 1(B) and (C)). Low percentages of microglia/macrophages (1.1%) and neurons (0.2%) were $TGF\alpha^+$ in sham brains, whereas 91.5% of microglia/macrophages and 76.6% of $MAP2^+$ neurons were $TGF\alpha^+$ three days after tMCAO (Figure 1(e)). These results strongly suggest an early elevation of TGFα in neurons and microglia/macrophages of the ischemic brain.

The TGFα receptor is widely distributed in CNS cells but is only upregulated in glial cells three days after ischemic stroke

Next, we used flow cytometry to examine the expression of EGFR on CNS cells. Consistent with previous

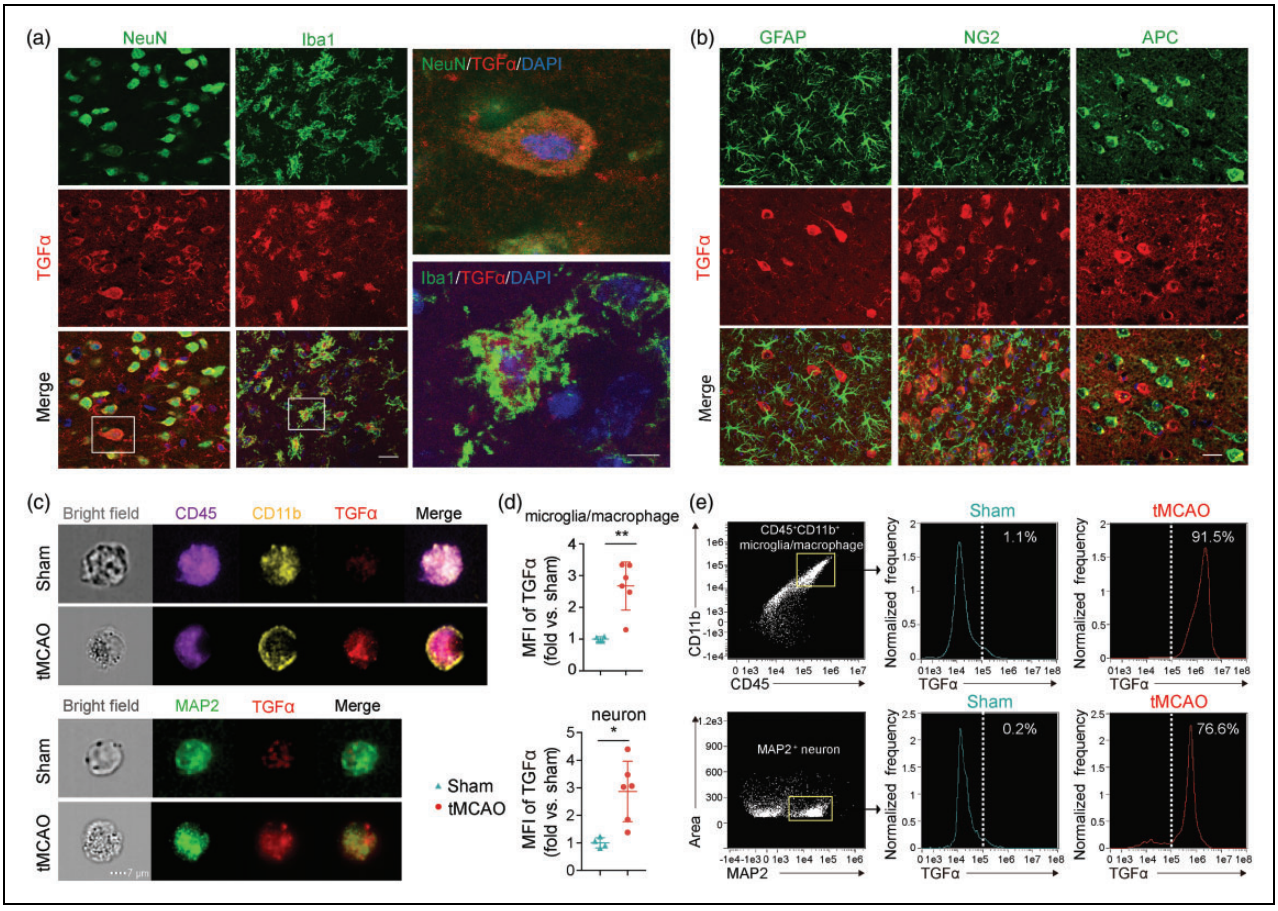

Figure 1. Ischemic injury increases TGFα expression in neurons and microglia within three days. C57/BL6 mice were subjected to transient (60 min) middle cerebral artery occlusion (tMCAO) and sacrificed three days later. (a) Representative confocal images showing colocalization of TGFα (red) in NeuN$^+$ (green) or Iba1$^+$ (green) cells in the ischemic brain. Nuclear staining with 4,6-diamidino-2-phenylindole (DAPI) is shown in blue. Scale bar: low magnification: 20 μm; high magnification: 5 μm. (b) Representative images of TGFα (red) and GFAP (green), NG2 (green), or APC (green) double labeling in the ischemic brain. Scale bar: 20 μm. (c–e) ImageStream images reveal increased TGFα expression in neurons and microglia/macrophages of the brain three days after stroke. Basal TGFα expression in sham control brains is low. (c) Representative images of TGFα expression in CD45$^+$CD11b$^+$ microglia/macrophages and MAP2$^+$ neurons and (d) Significant increase in mean fluorescent intensity (MFI) of TGFα in microglia/macrophages and neurons three days after tMCAO compared to sham control brains (two-tailed Student's *t* test). Data are expressed as fold change vs. sham. n = 4 for sham group and n = 6 for tMCAO group, *p<0.05; **p<0.01. (e) Representative plots showing expression of TGFα in CD45$^+$CD11b$^+$ microglia/macrophages or MAP2$^+$ neurons three days after tMCAO.

reports,[35] EGFR was widely expressed in many types of CNS cells, including CD45$^-$O4$^+$ oligodendrocyte linage cells, CD45$^+$CD11b$^+$ microglia/macrophages, CD45$^-$GLAST$^+$ astrocytes, and CD45$^-$NeuN$^+$ neurons (Figure 2(a) and (b)). Ischemic injury resulted in significant increases of EGFR expression in oligodendrocytes, microglia/macrophages, and astrocytes in the ischemic areas three days after tMCAO (Figure 2(b) and (c)). In contrast, the expression of EGFR on neurons remained unaffected by ischemic injury (Figure 2(b) and (c)). These results suggest that the receptor for TGFα is upregulated in microglial and other glial cells in the injured brain, but not in neurons.

TGFα deficiency worsens neurological scores and aggravates OPC and oligodendrocyte death three days after cerebral ischemia

To examine the functional role of TGFα in ischemic stroke, we subjected male WT and male TGFα KO mice to 60-min tMCAO (Figure 3(a)). In adherence with STAIR guidelines, rCBF was monitored before ischemia (baseline), during ischemia, and 10 min after reperfusion (Figure 3(b) and (c)). No significant difference in rCBF values between WT and TGFα KO mice was observed (Figure 3(c)). Thus, any differences between the two groups of animals could

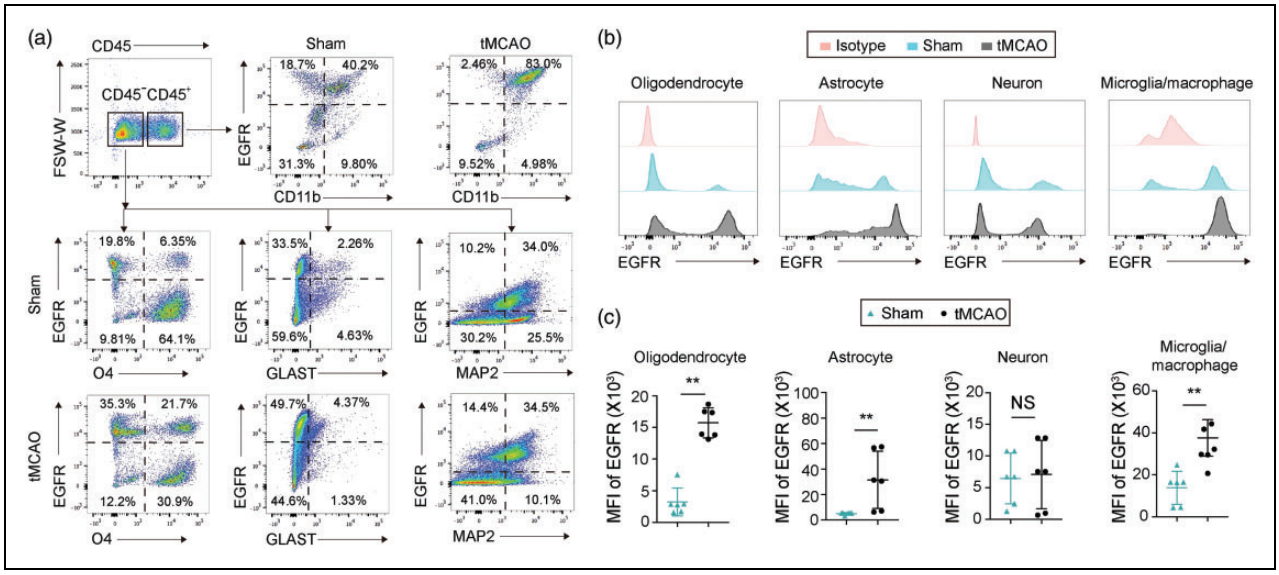

Figure 2. Ischemic injury increases expression of EGFR in oligodendrocytes, microglia/macrophages and astrocytes within three days. C57/BL6 mice were subjected to 60 min tMCAO or sham operation and sacrificed three days later. (a) Gating strategy of $CD45^+CD11b^+$ microglia/macrophages, $CD45^-O4^+$ oligodendrocyte lineage cells, $CD45^-GLAST^+$ astrocytes, and $CD45^-MAP2^+$ neurons in the ischemic brain. (b) Histograms showing EGFR expression on oligodendrocytes, astrocytes, neurons, and microglia/macrophages. Isotype antibodies were used as controls and (c) Quantification of mean fluorescence intensity (MFI) of EGFR in oligodendrocytes, astrocytes, neurons and microglia/macrophages. n = 6 per group. **$p<0.01$ by two-tailed Student's *t* test (normal distribution) or Mann–Whitney U test (non-normal distribution).

not be attributed to changes in the degree of initial ischemic insult.

The absence of TGFα worsened neurological deficits, as measured by a five-point neurological score at 1–3 days after stroke (Figure 3(d)), and enlarged infarct volumes three days after tMCAO (Figure 3(e) and (f)) compared to WT animals. Using TUNEL staining, we observed dramatic increases in the total number of $TUNEL^+$ dead/dying cells (Figure 3(h)) in TGFα KO mice three days after MCAO. Specifically, the numbers of dead/dying OPCs ($TUNEL^+PDGFR\alpha^+$, Figure 3(g) and (i), Supplemental Figure 2(A)) and oligodendrocytes ($TUNEL^+APC^+$, Figure 3(k) and (l), Supplemental Figure 2(B)) were both significantly increased in TGFα KO mice compared to WT mice. However, the total numbers of $PDGFR\alpha^+$ cells (Figure 3(j)) and APC^+ cells (Figure 3(m)) were not affected by TGFα deficiency three days after stroke.

TGFα deficiency exacerbates neurological deficits in both male and female mice after cerebral ischemia

Using an array of well-established behavioral tests, we explored the role of TGFα in long-term neurological function after stroke. Sham WT and sham TGFα KO mice exhibited no statistically significant differences in behavioral performance (Supplemental Figure 3(A) to (C)), and, therefore, data from these two sham groups were combined (Figure 4). Although the survival rate after stroke was slightly lower in TGFα KO mice compared to WT mice, the difference was not statistically significant (Figure 4(a)). TGFα deficiency exacerbated sensorimotor deficits after ischemic stroke, as demonstrated by increased latencies to contact (Figure 4(b)) and remove (Figure 4(c)) adhesive tape from the impaired forepaw as well as decreased latencies to fall off the accelerating Rotarod (Figure 4(d)).

We also assessed the role of TGFα in long-term neurological outcomes after stroke in female mice. Female mice were subjected to OVX two weeks prior to tMCAO to mimic the low estrogen conditions of menopause.[29,30] Similar to the aforementioned findings in male mice, the absence of TGFα expression in female mice exacerbated neurological deficits up to 14 days after tMCAO (Supplemental Figure 4(A) to (D)).

TGFα KO mice display long-term loss of white matter integrity

Next, we scrutinized the effects of TGFα on white mater integrity. We employed immunostaining for MBP and SMI32 as established markers of myelin integrity and pathologically exposed axons, respectively.[31] TGFα deficiency led to decreased MBP and increased SMI32 expression, resulting in an elevated SMI32/MBP ratio in both the striatum and cortex

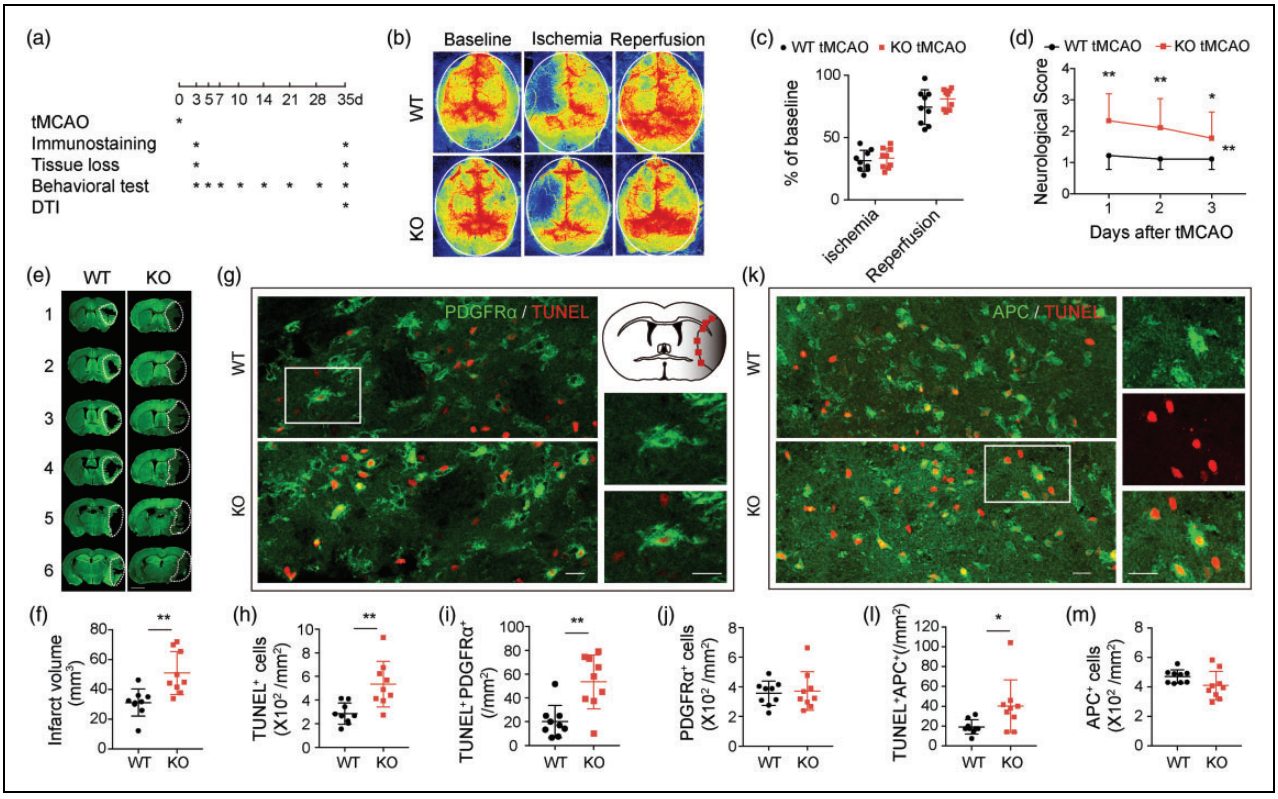

Figure 3. TGFα deficiency exacerbates OPC and oligodendrocyte death three days after ischemic injury. C57/BL6 wild-type and TGFα knockout (KO) mice were subjected to tMCAO and sacrificed three days later. (a) Experimental design. (b,c) Regional cerebral blood flow (rCBF) was monitored by laser speckle contrast imager before and during tMCAO and 10 min after reperfusion. Data were expressed as % of baseline before MCAO. n = 9 per group. (d) Neurological scores were measured 1–3 days after tMCAO. n = 9 per group, *p<0.05, **p<0.01 vs. WT, by two-way repeated measure ANOVA. (e,f) Infarct volumes were measured by MAP2 staining. White dotted lines encompass the infarct areas. Scale bar: 2 mm. n = 9 per group. **p<0.01, two-tailed Student's *t* test. (g–m) Quantification of dead/dying OPCs and oligodendrocytes in the peri-infarct areas of WT and TGFα KO mice three days after tMCAO. Representative images showing double immunofluorescent staining of PDGFRα (g, green) or APC (k, green) and TUNEL (red). Red squares illustrate the location of images in (g) and (k) in the ipsilateral peri-infarct regions. Scale bar: 20 μm. (h) Quantification of total dead/dying $TUNEL^+$ cells. (i) Quantification of $PDGFR\alpha^+TUNEL^+$ dead/dying OPCs. (j) Quantification of total $PDGFR\alpha^+$ OPCs. (l) Quantification of APC^+TUNEL^+ dead/dying oligodendrocytes and (m) Quantification of total APC^+ oligodendrocytes. n = 9 per group. *p<0.05, **p<0.01, by two-tailed Student's *t* test (normal distribution) or Mann–Whitney U test (non-normal distribution).

35 days after stroke (Figure 4(e) to (h)). Quantification of the MBP^+ area confirmed greater loss of white matter tissues in TGFα KO mice 35 days after tMCAO (Figure 4(i) and (j)). Furthermore, MBP loss was significantly correlated with longer latencies for adhesive tape removal (Figure 4(k)). The width of the ipsilateral EC was narrower in TGFα-deficient mice post stroke, compared with WT mice (Figure 4(l) and (m)).

DTI was used as a measure of white matter integrity by calculating the magnitude and directionality of water molecules within fiber tracts. Water molecules diffuse more freely along white matter tracts whereas myelination restricts diffusion perpendicular to the fasciculation.[36] Therefore, changes in diffusion anisotropy can be used to probe axonal integrity and myelination. Here, the DTI-derived diffusion measures are reported as a ratio of ipsilateral/contralateral values. Lower FA values were observed 35 days after stroke in the ipsilateral EC of TGFα KO mice vs. WT when compare to their respective contralateral ECs, indicating loss of integrity and connectivity of white matter (Figure 5(a) and (b)). RD was increased in TGFα KO mice (Figure 5(d)), most likely reflecting widespread demyelination in KO mice relative to WT mice. AD was also increased in TGFα KO mice, perhaps due to axonal damage and gliosis at later timepoints after stoke (Figure 5(c)).

Nodes of Ranvier are short regions between individual myelin internodes and contain sodium channels exposed to the extracellular space.[37] Contactin-associated protein (CASPR) and Na^+ channel 1.6 (NaV1.6) immunostaining was used to visualize

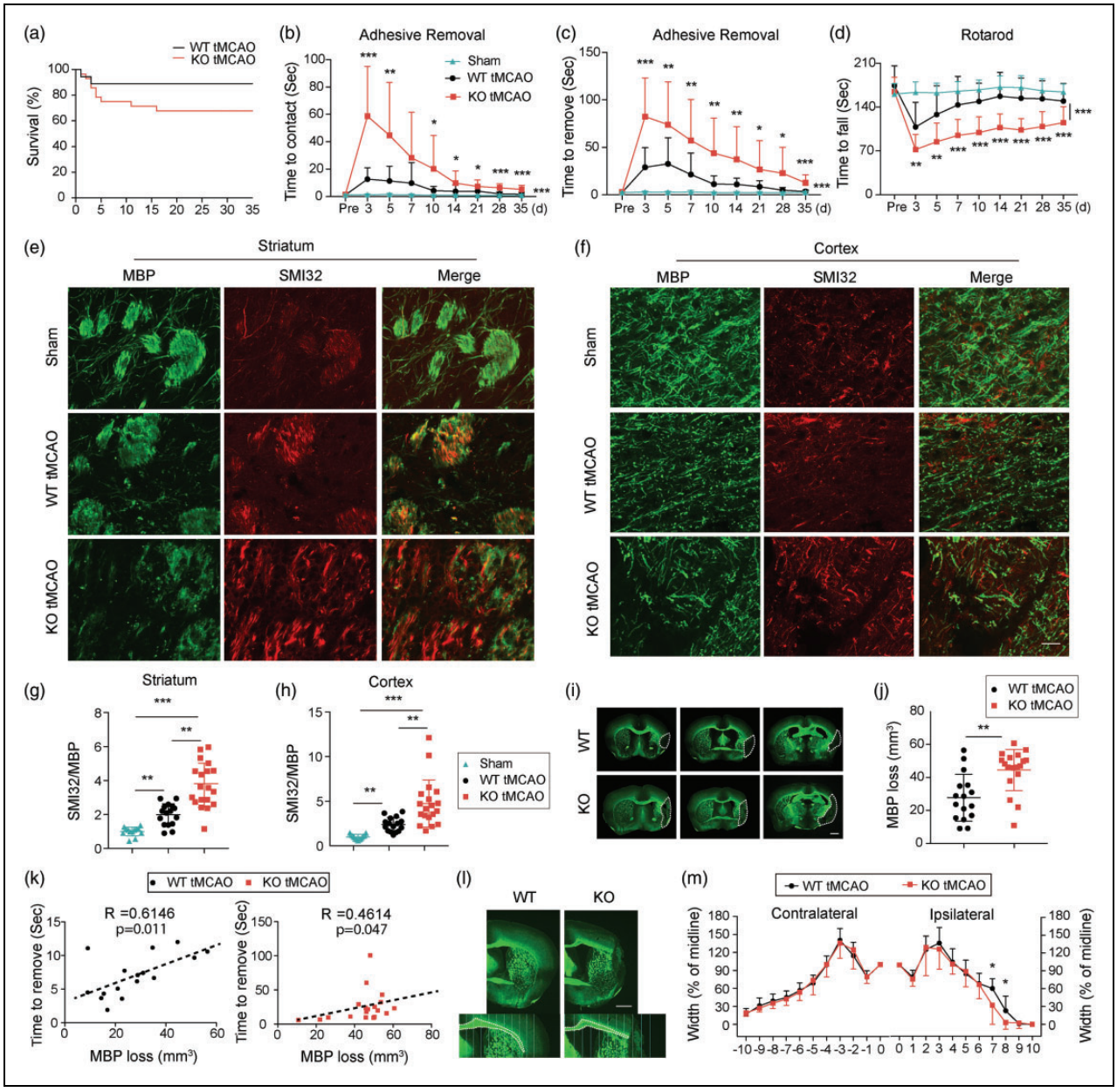

Figure 4. TGFα deficiency exacerbates behavioral deficits and impairs long-term white matter integrity 35 days after ischemic injury. C57/BL6 wild-type (WT) and TGFα knockout (KO) mice were subjected to tMCAO and were sacrificed 35 days later. (a) Survival rates after tMCAO in WT and TGFα KO mice. n = 22–28. Sensorimotor function was evaluated up to 35 days after tMCAO in WT and TGFα KO mice. (b,c) Adhesive removal test. Data are expressed as the latency to contact (b) and remove (c) the tape from the impaired forepaw. (d) Rotarod test. Data were expressed as the latency to fall off the rotating rod. n = 16–19, *p<0.05, **p<0.01, ***p<0.001 KO vs. WT; there are significant differences in KO vs. sham and WT vs. sham, according to the two way repeated-measures ANOVA followed by the Bonferroni post hoc. Double immunofluorescent staining for SMI32 (red) and MBP (green) in the striatum (e) and cortex (f) 35 days after tMCAO. Scale bar, 40 μm. Quantification of SMI32/MBP intensity ratio in the striatum (g) and cortex (h). Data were normalized to the signal intensity of sham brains. n = 13–19/group. **p<0.01, ***p<0.001; by Mann–Whitney U test. (i) Representative images of MBP-stained brain sections from WT and TGFα KO mice 35 days after tMCAO. Scale bar: 1 mm. (j) Quantification of tissue loss on MBP-stained brain sections. n = 16 in WT group, n = 19 in KO group. **p<0.01, by Mann–Whitney U test. (k) Correlation between MBP loss and the latency to remove the adhesive tape in WT (left, n = 16, Pearson test) and KO (right, n = 19, Spearman test) mice. (l) Representative images of MBP staining in the corpus callosum/external capsule. The corpus callosum/external capsule was divided into 10 equally spaced segments starting from the midline. Scale bar: 1 mm and (m) The width of the corpus callosum/external capsule in WT and TGFα KO mice was calculated as a percentage of the width at the midline. n = 13 in WT group, n = 14 in KO group. *p<0.05 vs. KO; by Mann–Whitney U test.

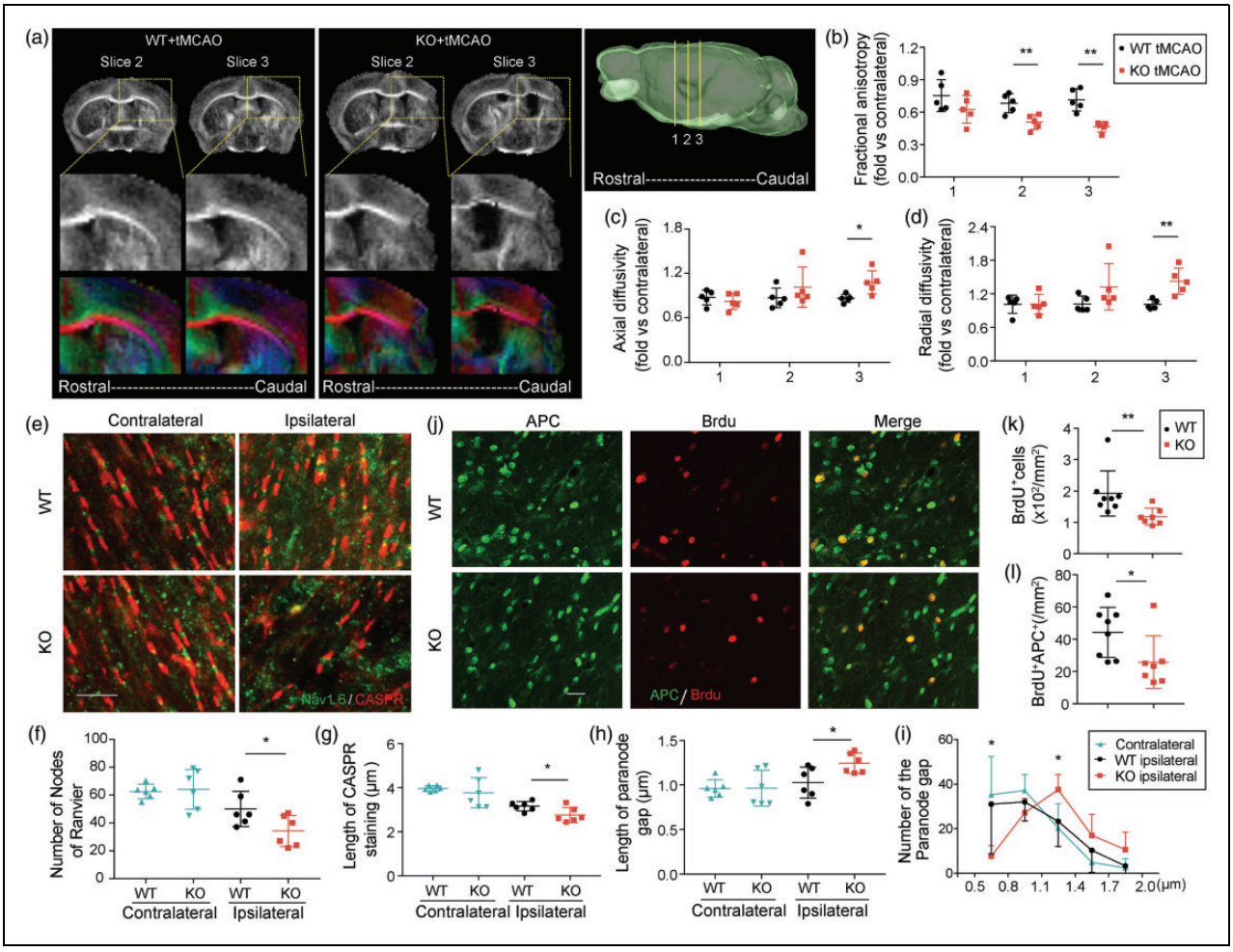

Figure 5. TGFα knockout mice display greater loss of white matter integrity and oligodendrogenesis failure after ischemic injury. (a) Representative images of DTI in WT and TGFα KO mice 35 days after tMCAO. (b–d) Quantification of fractional anisotropy (FA, b), axial diffusivity (AD, c), and radial diffusivity (RD, d) in external capsule areas. n = 5 per group. *p<0.05, **p<0.01; by two-tailed Student's *t* test. (e) Representative images of CASPR (red) and NaV1.6 (green) immunostaining in the external capsule (EC) of brain sections from WT and TGFα KO mice 35 days after stroke. Scale bar, 10 μm. (f) Quantification of the number of nodes of Ranvier in the EC. n = 6 per group. *p<0.05, by two-tailed Student's *t* test. Measurement of the lengths of CASPR stained regions (g) and immunonegative gaps between pairs of CASPR-stained regions (h). One hundred nodes were measured per mouse, n = 6 per group. *p<0.05, by two-tailed Student's *t* test. (i) The frequency histogram shows the number of nodes of Ranvier with respect to the length of paranode gap at 0.3 μm intervals for the contralateral EC or ipsilateral EC in WT or TGFα KO mice 35 days after stroke. *p<0.05, TGFα KO ipsilateral vs. WT ipsilateral; by Mann–Whitney U test. (j) Double immunofluorescent staining for BrdU (red) and APC (green) in the peri-infarct area 35 days after tMCAO. Scale bar: 20 μm. Number of total $BrdU^+$ cells (k) and $BrdU^+APC^+$ cells and (l) were quantified in the peri-infarct areas of WT and TGFα KO stroke mice. n = 7–8 per group. *p<0.05, **p<0.01, by Mann–Whitney U test.

paranodal and nodal lengths, respectively, in the CC and EC 35 days after stroke. In TGFα KO mice, the number of nodes of Ranvier was decreased (Figure 5(e) and (f)), the length of the region of CASPR immunostaining was shorter (Figure 5(e) and (g)), and the length between a pair of CASPR-immunostained regions was longer (Figure 5(e) and (h)). These collective findings indicate an elongation of the paranode gap in KO mice after stroke. Further analyses revealed an increased number of long paranode gaps and a reduced number of short paranode gaps in TGFα KO mice after stroke compared to WT (Figure 5(i)). In the contralateral control hemispheres, there were no significant differences between WT and KO mice in the number of nodes of Ranvier, the length of the CASPR-immunostained regions, or the length between a pair of CASPR-immunostained regions (Figure 5(f) to (h)). Furthermore, we observed reduced BrdU incorporation into APC^+ oligodendrocytes in TGFα KO mice 35 days after MCAO, suggesting a reduction in the number of

newly generated oligodendrocytes (Figure 5(j) and (k)). The total number of $BrdU^+$ cells was also reduced in TGFα KO mice (Figure 5(l)).

TGFα treatment reduces oligodendrocyte and OPC death after exposure to ischemic conditions in vitro

As the TGFα receptor EGFR is widely expressed in oligodendrocyte linage cells (Figure 2) and TGFα deficiency increases the number of dead/dying OPCs and oligodendrocytes (Figure 3(g) to (m)), we examined whether TGFα exerts direct effects on OPC/oligodendrocyte survival in vitro. Thus, cultured OPCs or oligodendrocytes were challenged with OGD, an in vitro model of ischemia, and incubated for 24 h in the presence or absence of TGFα (Figure 6(a)). Cell death was quantified by measuring LDH release into the culture media (Figure 6(b)). TGFα treatment at concentrations of 2.5, 5, 10, and 20 ng/mL significantly reduced OPC death, and treatment at 5, 10, and 20 ng/mL significantly reduced oligodendrocyte death, after OGD (Figure 6(b)). TGFα exerted minimal effects on non-OGD OPCs or oligodendrocytes at all concentrations tested (Figure 6(b)). Cell survival after OGD was also quantified by the MTT viability assay (Figure 6(c)) and Live/Dead staining (Figure 6(d) to (f)). The results of

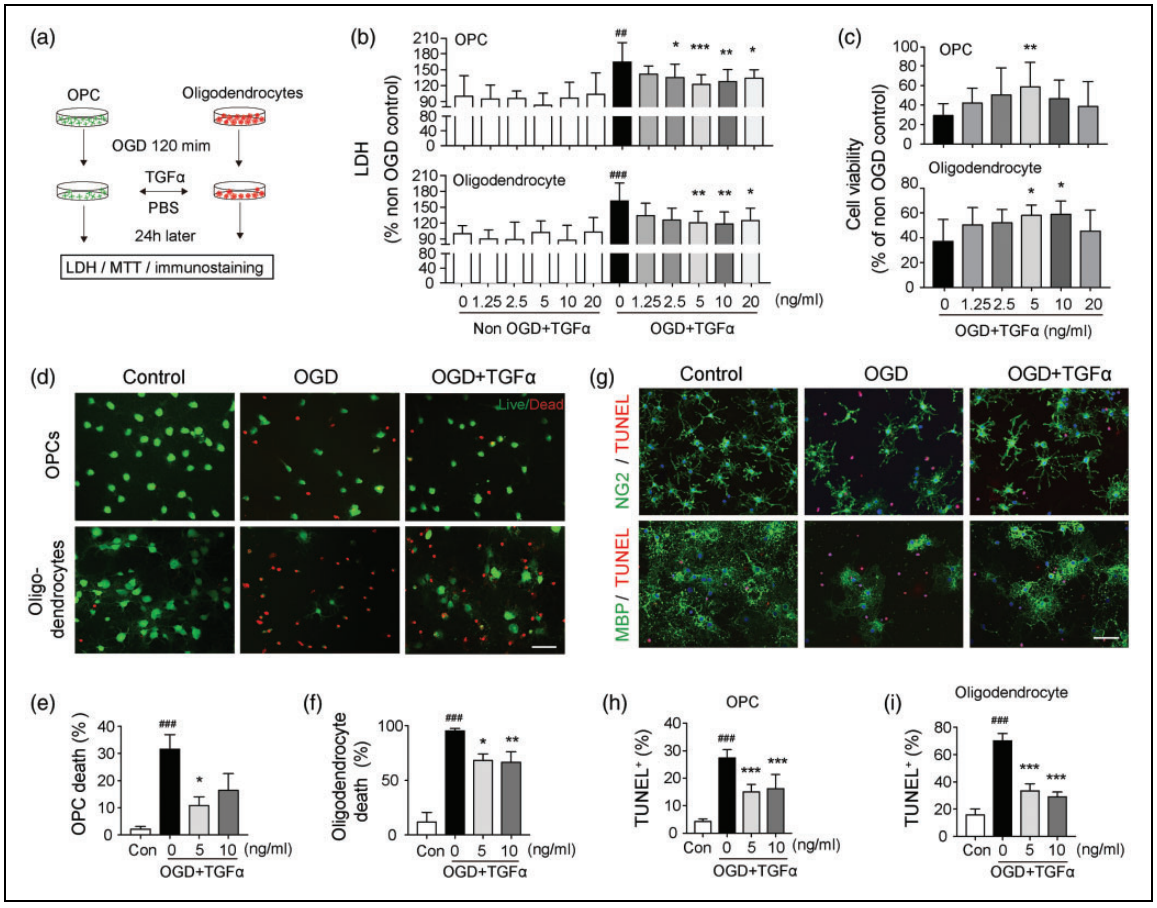

Figure 6. TGFα protects oligodendrocytes and OPCs against oxygen glucose deprivation-induced cell death in vitro. (a) Experimental design. Oligodendrocytes and OPCs were challenged with 120 min OGD, followed by TGFα or vehicle treatment for 24 h. The cultures were subjected to various stains (Live/Dead, TUNEL) combined with immunostaining for OPC and oligodendrocyte cell markers or the MTT assay. Culture media were collected for the LDH assay. (b) The LDH assay in culture media collected from OPC (upper) or oligodendrocyte cultures (lower), with or without OGD. (c) The MTT assay was performed at 24 h after OGD in OPC (upper) or oligodendrocyte cultures (lower). (d) Representative images of Live/Dead staining of cultured OPCs and oligodendrocytes. Healthy cells appear green and the dead cells appear red in this assay. Scale bar: 50 μm. Quantification of percentages of dead OPCs (e) and oligodendrocytes (f) by Live/Dead staining. Data are presented as % of total number of cells. (g) Representative images of NG2(green)/TUNEL(red) and MBP(green)/TUNEL(red) double-staining of OPCs or oligodendrocytes, respectively, 24 h after OGD. Scale bar: 50 μm. Quantification of percentages of $TUNEL^+$ cells in OPC (h) or oligodendrocyte and (i) cultures. Data are presented as % of total number of $DAPI^+$ cells. Data are mean ± SD from three independent experiments. *$p<0.05$, **$p<0.01$, ***$p<0.001$ vs. OGD without treatment; ##$p<0.01$, ###$p<0.001$ vs. non-OGD control; by one-way ANOVA.

both assays confirmed that the addition of TGFα at concentrations of 5 or 10 ng/mL significantly increased cell viability. Double staining of NG2 or MBP with TUNEL revealed a dramatic loss of viable $NG2^+$ OPCs or MBP^+ oligodendrocytes after OGD, and cellular viability was partially rescued by TGFα post-treatment (Figure 6(g)). TGFα significantly decreased the percentages of dead/dying $TUNEL^+$ cells after OGD in both OPC (Figure 6(h)) and oligodendrocyte cultures (Figure 6(i)). Although various viability/toxicity assays (LDH assay, MTT assay, Live/Dead staining and TUNEL staining) showed differences in sensitivity to detect cell death, they consistently demonstrated a protective effect of TGFα on OPCs at a concentration of 5 ng/mL, and on oligodendrocytes at 10 ng/ml. Therefore, 5 ng/mL and 10 ng/mL TGFα were used as optimal concentrations for OPC and oligodendrocytes, respectively, in subsequent experiments.

We observed a significant reduction in the numbers of newly generated oligodendrocytes in TGFα KO mice 35 days after tMCAO (Figure 5(j) to (l)). Given these findings, we also tested whether TGFα stimulates the differentiation of OPCs. According to the RT-PCR results, TGFα exerted no effect on the expression of mature oligodendrocyte genes (MBP, MOG, and MAG), suggesting a lack of direct effects on OPC differentiation (Supplemental Figure 5(A)). Furthermore, MBP and NG2 double staining was employed to confirm a lack of effect of TGFα on the percentage of MBP^+ oligodendrocytes in OPC cultures after two days of differentiation (Supplemental Figure 5(B) and (C)).

The transcription factor STAT3 mediates the protective effects of TGFα in OPCs and oligodendrocytes

STAT3 is an important mediator of signal transduction downstream of TGFα-EGFR engagement.[38] In our in vivo model, TGFα deficiency reduced the expression of p-STAT3—an indicator of STAT3 activation—in the ischemic brain three days after tMCAO (Figure 7(a) and (c)). The number of $pSTAT3^+Oligo2^+$ oligodendrocyte lineage cells was lower in TGFα KO mice three days after stroke, while the total number of $Oligo2^+$ cells remained the same in WT and KO mice (Figure 7(b) and (d)). Next, we measured the effect of TGFα on STAT3 activity in OGD-challenged OPCs and oligodendrocytes in vitro. Western blots revealed a fluctuation in p-STAT3 expression in OPCs at different time points after OGD. TGFα treatment significantly increased p-STAT3 levels in OPCs at 1 h after OGD (Figure 7(e) and (f)). In differentiated oligodendrocytes, there is a rapid decline in p-STAT3 levels after OGD, with a nadir at 1 h (Figure 7(e)). TGFα post-treatment elevated p-STAT3 expression in oligodendrocytes at 1 h after OGD (Figure 7(e) and (g)). To further investigate the involvement of the STAT3 pathway in the protective effects of TGFα in OPCs and oligodendrocytes, a specific STAT3 inhibitor (STAT3 inhibitor VI, Santa Cruz) was used to interrupt STAT3 activity. The LDH toxicity assay revealed that the STAT3 inhibitor promoted cell death even in the absence of OGD at a concentration of 25 μM for OPCs (Figure 7(h)) and 12.5 μM for oligodendrocyte (Figure 7(i)). A lower, non-toxic concentration of the STAT3 inhibitor (6.25 μM) abolished the protective effects of TGFα in OGD-challenged OPCs (Figure 7(h)) and oligodendrocytes (Figure 7(i)). NG2 or MBP and TUNEL double staining (Figure 7(j)) also revealed that co-administration of the STAT3 inhibitor diminished the oligoprotective effects of TGFα, increasing the number of $TUNEL^+$ cells (Figure 7(k) and (m)) and decreasing the number of $NG2^+$ cells (Figure 7(l)) or MBP^+ cells (Figure 7(n)) after OGD.

Discussion

White matter injury after stroke is characterized by the death of oligodendrocyte lineage cells and profound loss of myelin integrity.[39] The CNS myelin sheath maintains the normal function of enwrapped axons and provides metabolic support and substrates for axonal ATP synthesis.[40] In addition, an intact myelin sheath enables salutatory action potential propagation between nodes of Ranvier and speeds up neurotransmission along axons.[37] Thus, maintenance or restoration of myelin structure following CNS injury may limit axonal degeneration and facilitate functional recovery. Here, we report that TGFα is essential for structural maintenance of white matter after stroke. Lack of TGFα expression aggravated damage in cerebral white matter according to a number of outcome measurements, including DTI, loss of myelin sheath protein (MBP), and structural disruptions in the nodes of Ranvier. Furthermore, there was a positive correlation between loss of white matter integrity and long-term neurological deficits. These collective findings reveal a previously undefined function of TGFα in the maintenance of white matter integrity in the injured brain.

Improvements in white matter integrity after stroke may be achieved by protecting white matter components against ischemic injury and/or enhancing white matter repair and regeneration. In this study, we observed that TGFα protected OPCs and oligodendrocytes in the early stages of stroke, which may culminate in long-term improvements in white matter through multiple mechanisms. First, preservation of oligodendrocytes at acute stages after stroke may reduce the demyelination of axons and prevent further

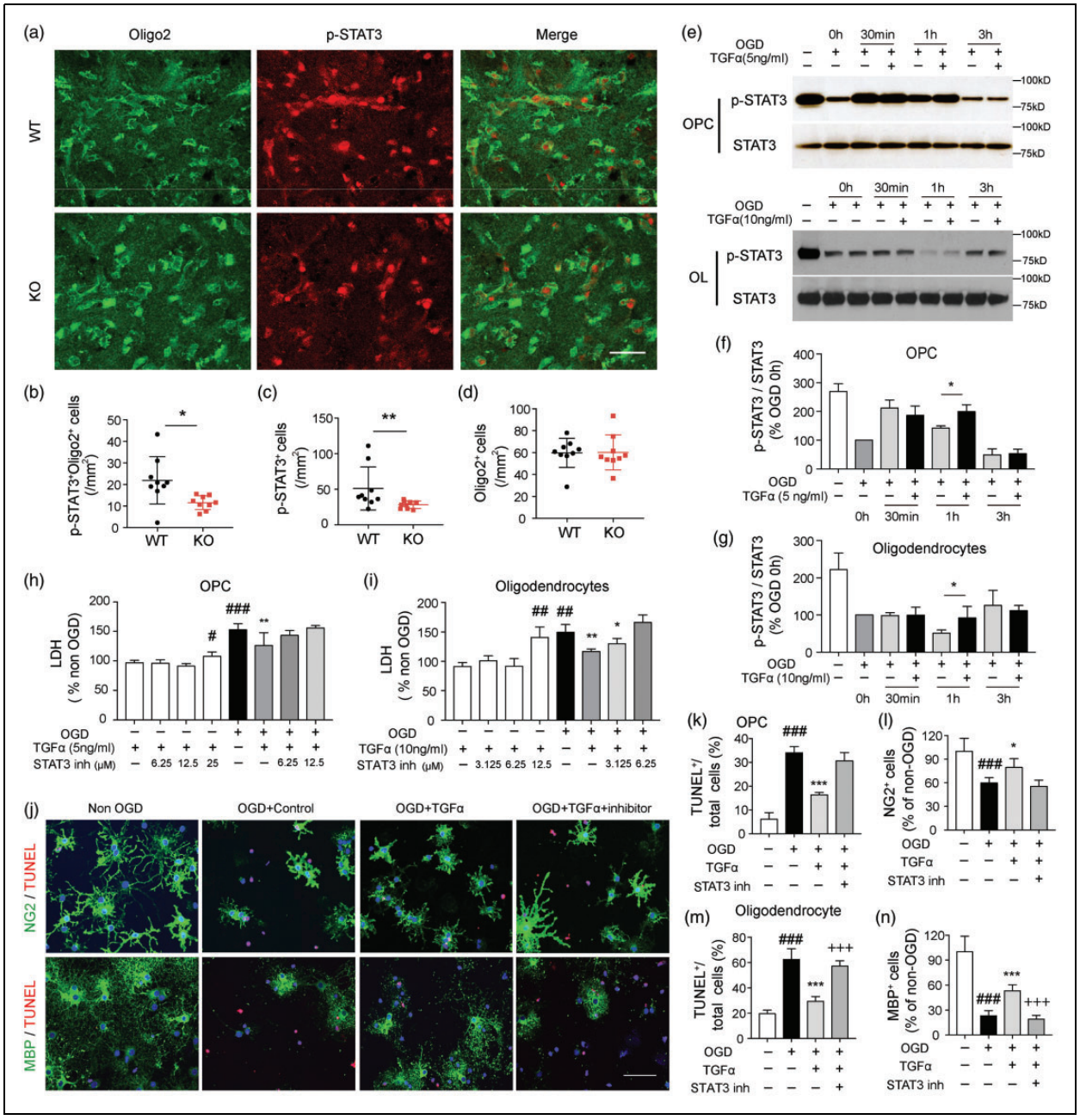

Figure 7. The transcription factor STAT3 mediates the protective effects of TGFα in OPCs and oligodendrocytes. (a–d) C57/BL6 wild-type (WT) and TGFα knockout (KO) mice were subjected to tMCAO and sacrificed three days later. (a) Representative image of Oligo2 (green) and p-STAT3 (red) immunostaining in WT and TGFα KO mice three days after MCAO. Scale bar, 40 μm. Quantification of p-STAT3$^+$Oligo2$^+$ cells (b, *p<0.05, by Student's *t* test), total p-STAT3$^+$ cells (c, **p<0.01, by Mann–Whitney U test) and Oligo2$^+$ cells (d) in WT and TGFα KO mice three days after tMCAO. (e–g) Cultured OPCs or oligodendrocytes were treated with TGFα after 2 h OGD. Western blot analyses of p-STAT3 and total STAT3 expression in OPCs (e,f) and oligodendrocytes (e,g) in non-OGD cells and at 0 h, 30 min, 1 h, and 3 h after OGD. Data were normalized to the 0 h OGD group. *p<0.05, by two-tailed Student's *t* test. (h–n) Cultured OPCs or oligodendrocytes were treated with TGFα with or without the specific STAT3 inhibitor at the indicated concentrations. LDH assay in the culture media collected from OPCs (h) and oligodendrocyte (i) cultures 24 h after OGD or non-OGD conditions. *p<0.05, **p<0.01; vs. OGD group; #p<0.01, ##p<0.01, ###p<0.001 vs. non-OGD control; by one-way ANOVA. (j) NG2 (green) or MBP (green) and TUNEL (red) double staining in OPCs and oligodendrocytes 24 h after OGD and various treatments. (j) Representative images of NG2/TUNEL (upper panel) and MBP/TUNEL (lower panel) double staining. Scale bar, 40 μm. Quantification of percentages of TUNEL$^+$ cells (k) and NG2$^+$ cells (l) in OPC cultures. Data are presented as % of total number of DAPI$^+$ cells. Quantification of percentages of TUNEL$^+$ cells (m) and MBP$^+$ cells and (n) in oligodendrocytes. Data are presented as % of total number of cells in non-OGD controls. Data are mean ± SD from three independent experiments. *p<0.05, ***p<0.001 vs. OGD; +++p<0.001 vs. OGD+TGFα group; ###p<0.001 vs. non-OGD control; by one-way ANOVA.

damage to other white matter structures. Second, the preservation of oligodendrocytes and their precursor cells appears to be a prerequisite for successful white matter regeneration. Myelin-producing oligodendrocytes are indispensable for remyelination and white matter repair after brain injuries. Evidence in models of remyelination suggests that both pre-existing oligodendrocytes and recently differentiated OPCs contribute to myelin repair. Indeed, a small number of OPCs persist throughout adulthood and constantly replenish the oligodendrocyte pool under physiological conditions.[41] Myelin production by newly differentiated OPCs is essential for the acquisition of new motor skills in mice.[42] In addition, fate mapping studies confirm that adult OPCs differentiate into myelinating oligodendrocytes in the context of neurodegeneration or demyelination.[43,44] In contrast, several human and animal studies suggest that the pre-existing mature oligodendrocytes, rather than newly generated oligodendrocytes, help maintain high myelin turnover rate in the normal brain and achieve myelin resynthesis under pathological conditions.[45,46] While the differentiation of OPCs is often arrested at premyelination stages in non-permissive environments in the compromised CNS,[47] reinitiating the myelination process in mature oligodendrocytes seems to be sufficient to increase myelin plasticity and enhance myelin repair.[46] Despite discrepancies in our knowledge of the source of myelin-producing oligodendrocytes in the injured brain, the protection of oligodendrocyte lineage cells is unequivocally critical in white matter repair. In our in vitro studies, we found that differentiated oligodendrocytes were more sensitive to OGD and demonstrated higher percentages of cell death upon the same duration of OGD challenge compared to OPCs. Interestingly, at higher concentrations, TGFα treatment exerted similar-sized protective effects (~50% rescue) on OPCs and oligodendrocytes against OGD. Our in vivo data demonstrated the importance of TGFα in the protection of pre-existing APC^+ oligodendrocytes. In addition, TGFα also protected OPCs against ischemic injury, which preserved the cellular reservoir for new oligodendrocytes. Therefore, TGFα may work in conjunction with other differentiating factors to enhance oligodendrogenesis after brain injuries. Consistent with this view, we showed that TGFα enhanced oligodendrocyte replacement after stroke (Figure 5(j) and (k)), although it had minimal direct effects on OPC differentiation in vitro (Supplemental Figure 5).

The results presented here are the first demonstration of the importance of STAT3 in TGFα-afforded oligodendrocyte protection against ischemia. STAT3 is well known for enhancing the proliferation and survival of malignant cells.[48] In physiological conditions and after exposure to cellular stress, activation of STAT3 encourages cell survival. For example, cardiac expression of STAT3 has been shown to protect cells against ischemia in the heart, by preserving mitochondrial complex I activity, reducing reactive oxygen species production, and inhibiting caspase-3 activation.[49] Activation of STAT3 signaling is also critical for neuronal survival after stimulation with IGF-1 and TNFα.[50] Previous studies report activation of STAT3 after TGFα/EGFR engagement, which mediates the growth of epithelial cells and some tumor cell lines.[51,52] Here, we report that TGFα deficiency inhibits STAT3 activity in oligodendrocyte lineage cells in the ischemic brain. In vitro studies further revealed that STAT3 activity after OGD in OPCs/oligodendrocytes was enhanced by TGFα treatment and inhibition of STAT3 activity completely abolished the protective effects of TGFα on OPCs/oligodendrocyte survival. Interestingly, the temporal profiles for STAT3 activity are different in OPCs and oligodendrocytes, suggesting different functions of this transcription factor during different developmental stages in the same cell lineage. TGFα is known to activate other signaling molecules, including ERK1/2[22] and C/ebpβ.[53] However, we did not observe changes in ERK1/2 in TGFα-treated OPC or oligodendrocytes (Supplemental Figure 6). C/ebpβ was below detection limit in OPC or oligodendrocytes without or with TGFα treatment.

Although the current study focused on the effects of TGFα on white matter components after stroke, it is important to acknowledge that TGFα may target multiple types of CNS cells. The flow cytometry data revealed that EGFR is widely expressed in different types of CNS cells, suggesting that the cellular targets of TGFα are not restricted to oligodendrocytes. TGFα has been reported to promote neuronal survival and enhance neurogenesis and angiogenesis in models of stroke and neurodegenerative diseases.[19,21,23–25,54,55] Consistent with those studies, we observed higher total numbers of $BrdU^+$ cells after stroke in TGFα-competent mice compared to TGFα KO mice, suggesting that TGFα affects regenerative events other than oligodendrogenesis. TGFα is known to directly stimulate astrocytes and transform them into a phenotype that supports neurite outgrowth after spinal cord injury.[56] Microglia-derived TGFα also regulates astrocyte activity and limits pathogenic glial actions during experimental autoimmune encephalomyelitis.[57] As the current study employed global TGFα KO mice, the observed deterioration in stroke outcomes indeed reflect collective protective effects of TGFα on multiple targets, rather than an exclusive effect on oligodendrocytes. In addition, the paucity of markers that are unique to OPCs makes it difficult to specifically label OPCs in histological immunostaining or flow cytometry. The two markers that we used for OPC labeling,

NG2 and PDGFRα, are both reportedly expressed in other types of CNS precursor cells.[58,59] However, the majority of PDGFRα/NG2 + cells do generate oligodendrocytes.[58,59] Furthermore, our in vitro data confirmed the direct effects of TGFα on oligodendrocyte lineage cells. Further studies using oligodendrocyte-specific EGFR KO mice are warranted to validate the effects of TGFα specifically on oligodendrocytes after ischemic stroke.

In conclusion, we have demonstrated that TGFα is an important endogenous protective factor for white matter and improves long-term functional recovery after stroke. These beneficial effects may partly be ascribed to the anti-apoptotic effects of TGFα in OPCs and oligodendrocytes. Additionally, TGFα may increase the pool of surviving OPCs that are available for regeneration of myelin-producing oligodendrocytes, thereby implementing endogenous myelin repair. Collectively, these results suggest that TGFα may be leveraged as a potential therapeutic strategy that emphasizes white matter preservation and reconstitution after stroke injury.

Authors' contributions

XD, Jie C, FX, JZ, WC, and ZS performed experiments and data analysis. XD contributed to manuscript writing. XH designed and supervised the study and wrote the manuscript. TKH and LMF performed magnetic resonance imaging study and contributed to editing of the manuscript. Jun C and RKL revised the manuscript.

Funding

The author(s) disclosed receipt of the following financial support for the research, authorship, and/or publication of this article: Xiaoming Hu is supported by a VA grant (I01 BX003651). Jun Chen is supported by VA grants (I01 BX0032495 and I01 BX003377). Jun Chen is a recipient of the VA Senior Research Career Scientist Award. Xuejiao Dai is supported by the University of Pittsburgh. This work benefitted from ImageStreamX MARKII grant NIH 1S10OD019942.

Declaration of conflicting interests

The author(s) declared no potential conflicts of interest with respect to the research, authorship, and/or publication of this article.

Supplementary material

Supplementary material for this paper can be found at the journal website: http://journals.sagepub.com/home/jcb

References

1. Liu H, Yang Y, Xia Y, et al. Aging of cerebral white matter. *Ageing Res Rev* 2017; 34: 64–76.
2. Pantoni L, Garcia JH and Gutierrez JA. Cerebral white matter is highly vulnerable to ischemia. *Stroke* 1996; 27: 1641–1646. (discussion 1647.
3. Fisher CM. Lacunes: small, deep cerebral infarcts. *Neurology* 2011; 77: 2104.
4. Baltan S, Besancon EF, Mbow B, et al. White matter vulnerability to ischemic injury increases with age because of enhanced excitotoxicity. *J Neurosci* 2008; 28: 1479–1489.
5. Zhao L, Biesbroek JM, Shi L, et al. Strategic infarct location for post-stroke cognitive impairment: a multivariate lesion-symptom mapping study. *J Cereb Blood Flow Metab* 2018; 38: 1299–1311.
6. Rost NS, Cougo P, Lorenzano S, et al. Diffuse microvascular dysfunction and loss of white matter integrity predict poor outcomes in patients with acute ischemic stroke. *J Cereb Blood Flow Metab* 2018; 38: 75–86.
7. Duncan ID, Brower A, Kondo Y, et al. Extensive remyelination of the CNS leads to functional recovery. *Proc Natl Acad Sci U S A* 2009; 106: 6832–6836.
8. Franklin RJ and Ffrench-Constant C. Remyelination in the CNS: from biology to therapy. *Nat Rev Neurosci* 2008; 9: 839–855.
9. Irvine KA and Blakemore WF. Remyelination protects axons from demyelination-associated axon degeneration. *Brain* 2008; 131: 1464–1477.
10. Domercq M, Sanchez-Gomez MV, Sherwin C, et al. System xc- and glutamate transporter inhibition mediates microglial toxicity to oligodendrocytes. *J Immunol* 2007; 178: 6549–6556.
11. Micu I, Jiang Q, Coderre E, et al. NMDA receptors mediate calcium accumulation in myelin during chemical ischaemia. *Nature* 2006; 439: 988–992.
12. Karadottir R, Cavelier P, Bergersen LH, et al. NMDA receptors are expressed in oligodendrocytes and activated in ischaemia. *Nature* 2005; 438: 1162–1166.
13. Marquardt H, Hunkapiller MW, Hood LE, et al. Rat transforming growth factor type 1: structure and relation to epidermal growth factor. *Science* 1984; 223: 1079–1082.
14. Lazar LM and Blum M. Regional distribution and developmental expression of epidermal growth factor and transforming growth factor-alpha mRNA in mouse brain by a quantitative nuclease protection assay. *J Neurosci* 1992; 12: 1688–1697.
15. Seroogy KB, Gall CM, Lee DC, et al. Proliferative zones of postnatal rat brain express epidermal growth factor receptor mRNA. *Brain Res* 1995; 670: 157–164.
16. Anchan RM, Reh TA, Angello J, et al. EGF and TGF-alpha stimulate retinal neuroepithelial cell proliferation in vitro. *Neuron* 1991; 6: 923–936.
17. Santa-Olalla J and Covarrubias L. Epidermal growth factor (EGF), transforming growth factor-alpha (TGF-alpha), and basic fibroblast growth factor (bFGF) differentially influence neural precursor cells of mouse embryonic mesencephalon. *J Neurosci Res* 1995; 42: 172–183.
18. Spranger M, Lindholm D, Bandtlow C, et al. Regulation of nerve growth factor (NGF) synthesis in the rat central nervous system: comparison between the effects of

interleukin-1 and various growth factors in astrocyte cultures and in vivo. *Eur J Neurosci* 1990; 2: 69–76.
19. Justicia C, Perez-Asensio FJ, Burguete MC, et al. Administration of transforming growth factor-alpha reduces infarct volume after transient focal cerebral ischemia in the rat. *J Cereb Blood Flow Metab* 2001; 21: 1097–1104.
20. Justicia C and Planas AM. Transforming growth factor-alpha acting at the epidermal growth factor receptor reduces infarct volume after permanent middle cerebral artery occlusion in rats. *J Cereb Blood Flow Metab* 1999; 19: 128–132.
21. Guerra-Crespo M, Sistos A, Gleason D, et al. Intranasal administration of PEGylated transforming growth factor-alpha improves behavioral deficits in a chronic stroke model. *J Stroke Cerebrovasc Dis* 2010; 19: 3–9.
22. Friguls B, Petegnief V, Justicia C, et al. Activation of ERK and Akt signaling in focal cerebral ischemia: modulation by TGF-alpha and involvement of NMDA receptor. *Neurobiol Dis* 2002; 11: 443–456.
23. Leker RR, Toth ZE, Shahar T, et al. Transforming growth factor alpha induces angiogenesis and neurogenesis following stroke. *Neuroscience* 2009; 163: 233–243.
24. Guerra-Crespo M, Gleason D, Sistos A, et al. Transforming growth factor-alpha induces neurogenesis and behavioral improvement in a chronic stroke model. *Neuroscience* 2009; 160: 470–483.
25. Alipanahzadeh H, Soleimani M, Soleimani Asl S, et al. Transforming growth factor-alpha improves memory impairment and neurogenesis following ischemia reperfusion. *Cell J* 2014; 16: 315–324.
26. Patel JR and Klein RS. Mediators of oligodendrocyte differentiation during remyelination. *FEBS Lett* 2011; 585: 3730–3737.
27. Xian CJ and Zhou XF. Roles of transforming growth factor-alpha and related molecules in the nervous system. *Mol Neurobiol* 1999; 20: 157–183.
28. Almeida SA, Claudio ER, Mengal V, et al. Exercise training reduces cardiac dysfunction and remodeling in ovariectomized rats submitted to myocardial infarction. *PLoS One* 2014; 9: e115970.
29. Verma R, Cronin CG, Hudobenko J, et al. Deletion of the P2X4 receptor is neuroprotective acutely, but induces a depressive phenotype during recovery from ischemic stroke. *Brain Behav Immun* 2017; 66: 302–312.
30. Li J, Siegel M, Yuan M, et al. Estrogen enhances neurogenesis and behavioral recovery after stroke. *J Cereb Blood Flow Metab* 2011; 31: 413–425.
31. Zhao J, Mu H, Liu L, et al. Transient selective brain cooling confers neurovascular and functional protection from acute to chronic stages of ischemia/reperfusion brain injury. *J Cereb Blood Flow Metab*. Epub ahead of print 18 October 2018. DOI: 10.1177/0271678X18808174.
32. Kim S, Steelman AJ, Koito H, et al. Astrocytes promote TNF-mediated toxicity to oligodendrocyte precursors. *J Neurochem* 2011; 116: 53–66.
33. Hu X, Zhang D, Pang H, et al. Macrophage antigen complex-1 mediates reactive microgliosis and progressive dopaminergic neurodegeneration in the MPTP model of Parkinson's disease. *J Immunol* 2008; 181: 7194–7204.
34. Li J, Ramenaden ER, Peng J, et al. Tumor necrosis factor alpha mediates lipopolysaccharide-induced microglial toxicity to developing oligodendrocytes when astrocytes are present. *J Neurosci* 2008; 28: 5321–5330.
35. Ferrer I, Alcantara S, Ballabriga J, et al. Transforming growth factor-alpha (TGF-alpha) and epidermal growth factor-receptor (EGF-R) immunoreactivity in normal and pathologic brain. *Progress Neurobiol* 1996; 49: 99–123.
36. Beaulieu C. The basis of anisotropic water diffusion in the nervous system – a technical review. *NMR Biomed* 2002; 15: 435–455.
37. Arancibia-Carcamo IL and Attwell D. The node of Ranvier in CNS pathology. *Acta Neuropathol* 2014; 128: 161–175.
38. Chan KS, Carbajal S, Kiguchi K, et al. Epidermal growth factor receptor-mediated activation of Stat3 during multistage skin carcinogenesis. *Cancer Res* 2004; 64: 2382–2389.
39. Shi H, Hu X, Leak RK, et al. Demyelination as a rational therapeutic target for ischemic or traumatic brain injury. *Exp Neurol* 2015; 272: 17–25.
40. Funfschilling U, Supplie LM, Mahad D, et al. Glycolytic oligodendrocytes maintain myelin and long-term axonal integrity. *Nature* 2012; 485: 517–521.
41. Young KM, Psachoulia K, Tripathi RB, et al. Oligodendrocyte dynamics in the healthy adult CNS: evidence for myelin remodeling. *Neuron* 2013; 77: 873–885.
42. McKenzie IA, Ohayon D, Li H, et al. Motor skill learning requires active central myelination. *Science* 2014; 346: 318–322.
43. Kang SH, Fukaya M, Yang JK, et al. NG2 + CNS glial progenitors remain committed to the oligodendrocyte lineage in postnatal life and following neurodegeneration. *Neuron* 2010; 68: 668–681.
44. Tripathi RB, Rivers LE, Young KM, et al. NG2 glia generate new oligodendrocytes but few astrocytes in a murine experimental autoimmune encephalomyelitis model of demyelinating disease. *J Neurosci* 2010; 30: 16383–16390.
45. Yeung MS, Zdunek S, Bergmann O, et al. Dynamics of oligodendrocyte generation and myelination in the human brain. *Cell* 2014; 159: 766–774.
46. Jeffries MA, Urbanek K, Torres L, et al. ERK1/2 Activation in preexisting oligodendrocytes of adult mice drives new myelin synthesis and enhanced CNS function. *J Neurosci* 2016; 36: 9186–9200.
47. Chang A, Tourtellotte WW, Rudick R, et al. Premyelinating oligodendrocytes in chronic lesions of multiple sclerosis. *N Engl J Med* 2002; 346: 165–173.
48. Laudisi F, Cherubini F, Monteleone G, et al. STAT3 interactors as potential therapeutic targets for cancer treatment. *Int J Mol Sci* 2018; 19(6): pii: E1787.
49. Zouein FA, Altara R, Chen Q, et al. Pivotal importance of STAT3 in protecting the heart from acute and chronic stress: new advancement and unresolved issues. *Front Cardiovasc Med* 2015; 2: 36.
50. Yadav A, Kalita A, Dhillon S, et al. JAK/STAT3 pathway is involved in survival of neurons in response to insulin-like growth factor and negatively regulated by

suppressor of cytokine signaling-3. *J Biol Chem* 2005; 280: 31830–31840.
51. Grandis JR, Drenning SD, Chakraborty A, et al. Requirement of Stat3 but not Stat1 activation for epidermal growth factor receptor-mediated cell growth in vitro. *J Clin Invest* 1998; 102: 1385–1392.
52. Song JI, Lango MN, Hwang JD, et al. Abrogation of transforming growth factor-alpha/epidermal growth factor receptor autocrine signaling by an RXR-selective retinoid (LGD1069, Targretin) in head and neck cancer cell lines. *Cancer Res* 2001; 61: 5919–5925.
53. Buck M, Poli V, van der Geer P, et al. Phosphorylation of rat serine 105 or mouse threonine 217 in C/EBP beta is required for hepatocyte proliferation induced by TGF alpha. *Mol Cell* 1999; 4: 1087–1092.
54. Mazzoni IE and Kenigsberg RL. Transforming growth factor alpha differentially affects GABAergic and cholinergic neurons in rat medial septal cell cultures. *Brain Res* 1996; 707: 88–99.
55. Cooper O and Isacson O. Intrastriatal transforming growth factor alpha delivery to a model of Parkinson's disease induces proliferation and migration of endogenous adult neural progenitor cells without differentiation into dopaminergic neurons. *J Neurosci* 2004; 24: 8924–8931.
56. White RE, Rao M, Gensel JC, et al. Transforming growth factor alpha transforms astrocytes to a growth-supportive phenotype after spinal cord injury. *J Neurosci* 2011; 31: 15173–15187.
57. Rothhammer V, Borucki DM, Tjon EC, et al. Microglial control of astrocytes in response to microbial metabolites. *Nature* 2018; 557: 724–728.
58. Zhu X, Hill RA, Dietrich D, et al. Age-dependent fate and lineage restriction of single NG2 cells. *Development* 2011; 138: 745–753.
59. Rivers LE, Young KM, Rizzi M, et al. PDGFRA/NG2 glia generate myelinating oligodendrocytes and piriform projection neurons in adult mice. *Nat Neurosci* 2008; 11: 1392–1401.